J Arid Land (2023) 15(5): 545–561
https://doi.org/10.1007/s40333-023-0056-x

Science Press Springer-Verlag

Quantifying major sources of uncertainty in projecting the impact of climate change on wheat grain yield in dryland environments

Reza DEIHIMFARD[1], Sajjad RAHIMI-MOGHADDAM[2*], Farshid JAVANSHIR[1], Alireza PAZOKI[3]

[1] Department of Agroecology, Environmental Sciences Research Institute, Shahid Beheshti University, Tehran 19839–69411, Iran;
[2] Department of Production Engineering and Plant Genetics, Faculty of Agriculture and Natural Resources, Lorestan University, Khorramabad 68151–44316, Iran;
[3] Department of Agrotechnology, Yadegar-e-Imam Khomeini (RAH) Shahre Rey Branch, Islamic Azad University, Tehran 18151–63111, Iran

Abstract: Modelling the impact of climate change on cropping systems is crucial to support policy-making for farmers and stakeholders. Nevertheless, there exists inherent uncertainty in such cases. General Circulation Models (GCMs) and future climate change scenarios (different Representative Concentration Pathways (RCPs) in different future time periods) are among the major sources of uncertainty in projecting the impact of climate change on crop grain yield. This study quantified the different sources of uncertainty associated with future climate change impact on wheat grain yield in dryland environments (Shiraz, Hamedan, Sanandaj, Kermanshah and Khorramabad) in eastern and southern Iran. These five representative locations can be categorized into three climate classes: arid cold (Shiraz), semi-arid cold (Hamedan and Sanandaj) and semi-arid cool (Kermanshah and Khorramabad). Accordingly, the downscaled daily outputs of 29 GCMs under two RCPs (RCP4.5 and RCP8.5) in the near future (2030s), middle future (2050s) and far future (2080s) were used as inputs for the Agricultural Production Systems sIMulator (APSIM)-wheat model. Analysis of variance (ANOVA) was employed to quantify the sources of uncertainty in projecting the impact of climate change on wheat grain yield. Years from 1980 to 2009 were regarded as the baseline period. The projection results indicated that wheat grain yield was expected to increase by 12.30%, 17.10%, and 17.70% in the near future (2030s), middle future (2050s) and far future (2080s), respectively. The increases differed under different RCPs in different future time periods, ranging from 11.70% (under RCP4.5 in the 2030s) to 20.20% (under RCP8.5 in the 2080s) by averaging all GCMs and locations, implying that future wheat grain yield depended largely upon the rising CO_2 concentrations. ANOVA results revealed that more than 97.22% of the variance in future wheat grain yield was explained by locations, followed by scenarios, GCMs, and their interactions. Specifically, at the semi-arid climate locations (Hamedan, Sanandaj, Kermanshah and Khorramabad), most of the variations arose from the scenarios (77.25%), while at the arid climate location (Shiraz), GCMs (54.00%) accounted for the greatest variation. Overall, the ensemble use of a wide range of GCMs should be given priority to narrow the uncertainty when projecting wheat grain yield under changing climate conditions, particularly in dryland environments characterized by large fluctuations in rainfall and temperature. Moreover, the current research suggested some GCMs (e.g., the IPSL-CM5B-LR, CCSM4, and BNU-ESM) that made moderate effects in projecting the impact of climate change on wheat grain yield to be used to project future climate conditions in similar environments worldwide.

*Corresponding author: Sajjad RAHIMI-MOGHADDAM (E-mail: rahimi.s@lu.ac.ir)
Received 2022-08-19; revised 2023-01-08; accepted 2023-01-28

Keywords: wheat grain yield; climate change; Agricultural Production Systems sIMulator (APSIM)-wheat model; General Circulation Models (GCMs); arid climate; semi-arid climate; Iran

Citation: Reza DEIHIMFARD, Sajjad RAHIMI-MOGHADDAM, Farshid JAVANSHIR, Alireza PAZOKI. 2023. Quantifying major sources of uncertainty in projecting the impact of climate change on wheat grain yield in dryland environments. Journal of Arid Land, 15(5): 545–561. https://doi.org/10.1007/s40333-023-0056-x

1 Introduction

Wheat is counted among the "big three" cereal crops in the world, with over 0.219×10^9 hm^2 of land harvested annually (FAO, 2020). Crops will be substantially affected by climate change in the future (Liu et al., 2021; Obembe et al., 2021). Hence, it is essential to accurately project future climate change so as to assess its impacts on crop grain yield (especially on wheat grain yield), since a small bias in the projection of climate variables is likely to result in significant variations in predicting the phenological development and final grain yield of crops (Ruiz-Ramos et al., 2016; Wang et al., 2018). General Circulation Models (GCMs) accompanied by crop simulation models have been broadly applied to investigate the impact of future climate change on different crop grain yields all around the world (Asseng et al., 2013; Tao et al., 2018; Rahimi-Moghaddam et al., 2019). They are useful tools for assessing the impact of climate change in a low-cost and time-saving way. One major problem, however, is that using GCMs under various greenhouse gas emission scenarios (i.e., representative concentration pathways (RCPs)) and future time periods (i.e., 2030s, 2050s and 2080s) across different climate types is associated with uncertainty (Wang et al., 2018). Uncertainty is defined as a state of incomplete knowledge resulted from a lack of information or disagreement about what is known; it has many types of sources, e.g., imprecision of the data, ambiguously defined concepts or terminology, uncertain projections of human activities, etc. (Edenhofer, 2014). Substantial uncertainty can result from model resolution at different spatiotemporal scales, model parameterization, model structure, and downscaling methods (Asseng et al., 2013; Eghdamirad et al., 2017; Hosseinzadehtalaei et al., 2017; Chapagain et al., 2022).

Previous studies have indicated that the uncertainty in the assessments of climate change impact was related to climate models (Kassie et al., 2015), greenhouse gas emission scenarios (Shi et al., 2020), crop models (Asseng et al., 2013), downscaling methods (Khan et al., 2006), future time periods (Hawkins et al., 2016), and soil types (Wang et al., 2018). According to a simulation study in Ethiopia (Kassie et al., 2015), for example, the uncertainty arising from GCMs was about –28.00% to –8.00% higher than those between GCMs and crop models (–20.00% to –19.00%) and between GCMs and RCPs (–22.00% to –17.00%). A similar study in southeastern Australia concluded that the major factors affecting the uncertainty in projecting drought were the GCMs, with the variability values of 19.20%–53.00%, followed by their interaction with RCPs, with the variability values of 17.20%–44.30% (Shi et al., 2020). Rettie et al. (2022) assessed the impact of climate change on wheat growth in Ethiopia based on a multi-model uncertainty analysis and reported that the uncertainty in wheat grain yield changes was largely dominated by the variations in the crop models (with the coefficient of variation (CV) values of 71.00%–80.00%), followed by climate models (with the CV values of 11.00%–25.00%). It is also important to assess the sources of uncertainty in the assessment of different climate types in agricultural research, particularly for the management practices, such as developing suitable adaptation strategies to mitigate the impact of climate change on crop grain yield.

The uncertainty associated with projecting the impact of climate change on crop yield stems not only from the above-mentioned sources, but also from the climate conditions studied (Olesen et al., 2007). A global-scale study reported that 17 GCMs collectively underestimated (–4.00% to –2.00%) the mean annual maximum temperature in arid and semi-arid regions of the Sahara and the southwestern region of the United States, which are most subject to severe heat waves and droughts (Cheng et al., 2015). The results also showed that the majority of GCMs tended to underestimate the historical annual maximum temperature in the United States and Greenland,

while there is widespread disagreement in their simulations over cold regions. In another global-scale study (Freychet et al., 2021), researchers have predicted that the climatological bias in the difference between hot days (the number of days above the daily climatological 98th percentile during the warm season) and normal days in GCMs caused an underestimation of the frequency of unusually hot days in many low-latitude areas such as tropical regions (1.00%–48.00%) and Southeast Asia (1.00%–22.00%) in the future. These biases could lead to uncertainty in future crop yield projection. For example, Rahman et al. (2018) assessed the uncertainty in projecting the impact of climate change on cotton production in Pakistan, and found large variations in projected climatic variables (increases of 3.80% to 12.40% for mean temperature and changes of –8.00% to 22.00% for rainfall in the future period compared to the baseline period) under different GCM projections, RCPs, and future time periods. Accordingly, these uncertainties resulted in a large variability of cotton seed yield prediction (–70.00% to 4.00%).

The current research was conducted to quantify the major sources of uncertainty when projecting the impact of climate change on wheat grain yield in dryland environments with arid and semi-arid climates, where the ratio of mean annual rainfall to mean annual potential evapotranspiration (i.e., Aridity Index) varies from 0.05 to 0.20 for arid climate and 0.20 to 0.50 for semi-arid climate (UNEP, 1992; Amiri et al., 2016). Specifically, the downscaled daily outputs of 29 GCMs under RCP4.5 and RCP8.5 scenarios in the near future (2030s), middle future (2050s), and far future (2080s) were used as inputs for the Agricultural Production Systems sIMulator (APSIM)-wheat model. Also, the current research focused on introducing some GCMs that make moderate effects in projecting the impact of climate change on wheat grain yield to be used to project future climate conditions in similar environments worldwide.

2 Materials and methods

2.1 Study area and data sources

The current research focused on five provinces (Fars, Hamedan, Kurdistan, Kermanshah, and Lorestan) in eastern and southern Iran, which account for approximately 42.00% (i.e., 1.40×10^6 hm^2) of the total global dryland wheat planting area. We selected one representative location from each province based on climate diversity and cultivated area. We then categorized the selected five representative locations (Shiraz, Hamedan, Sanandaj, Kermanshah and Khorramabad) into three climate classes (arid cold, semi-arid cold and semi-arid cool; Table 1) according to the agroclimatic classification defined by the United Nations Educational, Scientific and Cultural Organization (UNESCO) (UNESCO, 1979; De Pauw et al., 2018). Long-term (1980–2009) monthly climate characteristics of the five representative locations are shown in Table 2.

Long-term (1980–2009) meteorological records for the five representative locations were obtained from Agricultural Meteorological Organization of Iran (www.irimo.ir). Climate data included daily solar radiation (MJ/(m^2·d)), maximum temperature (°C), minimum temperature (°C), and rainfall (mm). Soil property data of depth (mm), bulk density (BD; g/m^3),

Table 1 Climate classes and soil properties of the five representative locations

Location	Climate class	Latitude	Longitude	Altitude (m a.s.l.)	BD (g/m^3)	CLL (mm/mm)	DUL (mm/mm)	SAT (mm/mm)	Cultivated area (×10^3 hm^2)
Shiraz	Arid cold	29°36′37″N	52°31′52″E	1585	1.30×10^{-6}	0.23	0.39	0.51	13.50
Hamedan	Semi-arid cold	34°47′57″N	48°30′52″E	1850	1.35×10^{-6}	0.19	0.35	0.49	45.60
Sanandaj	Semi-arid cold	35°18′53″N	46°59′55″E	1500	1.33×10^{-6}	0.26	0.39	0.50	41.10
Kermanshah	Semi-arid cool	34°18′51″N	47°03′54″E	1400	1.37×10^{-6}	0.13	0.31	0.48	8.30
Khorramabad	Semi-arid cool	33°27′59″N	48°21′20″E	1147	1.33×10^{-6}	0.22	0.37	0.50	38.00

Note: BD, bulk density; CLL, crop lower limit of water availability; DUL, drained upper limit; SAT, saturated water content.

Table 2 Long-term (1980–2009) monthly and annual climate characteristics of the five representative locations

Location	Jan	Feb	Mar	Apr	May	Jun	Jul	Aug	Sep	Oct	Nov	Dec	Annual
	Maximum temperature (°C)												
Shiraz	12.50	15.10	19.00	24.80	31.30	36.50	38.40	37.70	34.10	28.20	20.50	15.00	26.09
Hamedan	3.00	5.60	12.00	18.30	23.60	30.40	34.30	34.10	29.30	21.70	13.20	6.30	19.32
Sanandaj	6.20	8.40	14.10	20.30	25.90	33.20	37.30	37.00	32.20	24.50	15.40	9.30	21.98
Kermanshah	9.30	10.80	14.90	20.70	27.20	33.10	36.40	36.00	31.70	25.00	16.60	11.70	22.78
Khorramabad	10.50	12.60	16.90	22.50	28.70	35.70	39.30	39.00	34.60	27.40	18.80	12.70	24.89
Location	Minimum temperature (°C)												
Shiraz	0.40	2.20	5.50	9.90	14.70	18.60	21.30	20.40	15.80	10.60	5.40	1.70	10.54
Hamedan	–8.10	–5.70	–0.70	4.30	7.40	10.70	14.20	13.00	7.90	4.10	0.00	–4.60	3.59
Sanandaj	–5.50	–4.00	0.20	4.90	8.60	12.70	17.40	16.50	10.20	6.20	1.40	–2.90	5.48
Kermanshah	0.30	1.20	4.50	9.40	14.50	19.10	22.40	22.00	17.80	13.00	6.20	2.20	11.05
Khorramabad	–0.90	0.30	3.20	7.20	10.60	14.40	18.60	17.80	12.90	9.10	4.20	0.70	8.17
Location	Mean temperature (°C)												
Shiraz	6.45	8.65	12.25	17.35	23.00	27.55	29.85	29.05	24.95	19.40	12.95	8.35	18.32
Hamedan	–2.55	–0.05	5.97	11.30	15.50	20.55	24.25	23.55	18.60	12.90	6.60	0.85	11.46
Sanandaj	0.35	2.20	7.15	12.60	17.25	22.95	27.35	26.75	21.20	15.35	8.40	3.20	13.73
Kermanshah	4.80	6.00	9.70	15.05	20.85	26.10	29.40	29.00	24.75	19.00	11.40	6.95	16.92
Khorramabad	4.80	6.45	10.05	14.85	19.65	25.05	28.95	28.40	23.75	18.25	11.50	6.70	16.53
Location	Cumulative rainfall (mm)												
Shiraz	80.20	53.60	53.80	21.40	5.80	0.20	0.40	1.10	0.00	3.60	30.50	70.30	320.90
Hamedan	29.50	33.70	44.50	38.00	20.70	2.60	2.70	1.90	1.00	22.80	32.70	34.90	265.00
Sanandaj	52.10	59.00	68.50	66.10	32.70	2.10	1.00	0.10	0.80	34.40	65.90	53.50	436.20
Kermanshah	109.10	84.90	98.30	58.70	16.50	0.10	0.50	0.90	1.20	36.20	81.90	80.80	569.10
Khorramabad	57.60	66.40	71.70	54.50	18.90	1.00	0.20	0.10	0.60	20.70	48.40	70.40	410.50

particle size distribution (silt, sand and clay; %) and organic carbon (OC; %) were also obtained from the Agricultural Meteorological Organization of Iran (www.irimo.ir), which were used to estimate soil parameters required by the crop model. Soil parameters included drained upper limit (DUL; mm/mm), crop lower limit of water availability (CLL; mm/mm) and saturated water content (SAT; mm/mm). The study adopted the soil-plant-air-water (SPAW) model to estimate soil parameters based on pedotransfer functions (Saxton and Willey, 2005) and soil property data (depth, BD, particle size distribution and OC), since the measurements of DUL, CLL and SAT could be a time-consuming and tedious process.

Local management practices (e.g., sowing window and depth, tillage method, initial soil water and nitrogen application) at each location were obtained from local experts at the Ministry of Agriculture and the Agricultural and Natural Resources Research and Education Center, Iran as well as the previous study of Rahimi-Moghaddam et al. (2021). Sowing depth (5.00 cm), tillage method (conventional cultivation) and nitrogen application (180.00 kg N/hm^2) were held constant throughout all simulations. According to local practices, farmers apply half of nitrogen fertilizer at sowing time and the other half at stem elongation time. The sowing window was from 23 September to 23 November and the average initial soil water was 30.00 mm across the five representative locations. All simulations were carried out under water-limited conditions with no other abiotic or biotic constraints.

2.2 Crop model

The Agricultural Production Systems sIMulator (APSIM)-wheat model version 7.7 (Holzworth et al., 2014) was used in this study. The model can capture the effects of environmental changes and management practices on crop growth and development on a daily time scale. The inputs required to run the model consist of daily climate variables, soil parameters, genetic coefficients for each cultivar and management data to simulate crop growth and development, leaf area index, water-nitrogen balance and grain yield (Holzworth et al., 2014). Biomass accumulation is a function of photosynthetic active radiation intercepted by canopy and radiation use efficiency (RUE). RUE is affected by temperature, phenological stage, CO_2 concentration and nitrogen level. Temperature is a function of the daily mean temperature linearly interpolated by the APSIM-wheat model, which affects RUE from sowing to harvest time. Increasing CO_2 concentration can enhance transpiration efficiency (TE) and RUE through the factors of $f_{C,TE}$ and $f_{C,RUE}$, respectively. $f_{C,TE}$ is the CO_2 factor for TE, which is a function of CO_2 concentration and linearly increases from 1.00 to 1.37 when CO_2 concentration rises from 350.00 to 700.00 mg/L. $f_{C,RUE}$ is the CO_2 factor affecting the RUE of C_3 plants (e.g., wheat), which can be calculated by a function of CO_2 concentration (C; mg/L), temperature dependent CO_2 compensation point (C_i; mg/L) and daily mean temperature (T_{mean}; °C) as follows (Reyenga et al., 1999):

$$f_{C,RUE} = \frac{(C - C_i)(350 + 2C_i)}{(C + 2C_i)(350 - C_i)}, \tag{1}$$

$$C_i = \frac{163 - T_{mean}}{5 - 0.1T_{mean}}. \tag{2}$$

The phenological stages in the APSIM-wheat model are mainly driven by the accumulations of thermal time. Each stage has a fixed thermal time limit, which can be adjusted on the basis of the phase under consideration, using cultivar specific parameters (e.g., vernalization and photoperiod sensitivity). Both photoperiod and vernalization affect the development rate between the emergence and floral initiation of plants. Partitioning of the assimilates into different plant organs is based on partitioning coefficients that vary in different phenological stages.

The APSIM-wheat model can also capture the impact of extreme temperature on wheat growth and grain yield using the heat-shock module embedded in this model. The impact of extreme temperature on grain number and grain size can be estimated using sensitivity factors, ranging from 0.00 to 1.00. The effect of daily maximum temperature on grain number (when daily maximum temperature higher than 26.00°C) and the number of days required to consider the effect (7 d) before and after anthesis can also be captured in the heat-shock module. Further details regarding the heat-shock module in the APSIM-wheat model can be found in Lobell et al. (2015).

Soil-water balance in the APSIM-wheat model was projected on a daily scale, taking into account soil evaporation, plant transpiration, drainage and runoff, and based on water inputs from rainfall and irrigation. We calculated each process individually according to the relationships introduced to the APSIM-wheat model. Crop transpiration, for instance, was projected by potential crop growth rate, potential biomass accumulation and TE. Runoff was determined through the United States Department of Agriculture (USDA) curve number (Boughton, 1989; Ponce and Hawkins, 1996; Hawkins et al., 2008). Additional details about the APSIM-wheat model can be found in Holzworth et al. (2014) and the APSIM website (http://www.apsim.info/).

So far, the APSIM-wheat model has been applied successfully as a powerful tool to assess the impact of future climate change on wheat grain yield under different climate types in Iran (Rahimi-Moghaddam et al., 2019) and other countries (Araya et al., 2015; Wang et al., 2018; Saddique et al., 2020). Moreover, the model has also been previously used in many scientific reports for sensitivity and uncertainty analysis to predict crop grain yield (Zhao et al., 2014; Hao et al., 2021; Collins et al., 2022; Vogeler et al., 2022). In this study, we adopted 'Azar-2', the most commercial and dominant dryland wheat cultivar in Iranian dryland agro-ecosystem, as a case study. The APSIM-wheat model was calibrated for this cultivar to obtain the genetic

cultivar-specific parameters (Table 3) required for the model and validated across six locations for 13 seasons in dryland environments (Rahimi-Moghaddam et al., 2021) (Supplementary Table S1).

Table 3 Description of the parameters in the APSIM-wheat model used to predict the grain yield of 'Azar-2' cultivar

Parameter	Unit	Value
Thermal time at the end of juvenile stage	°Cd	380.00
Number of grains per gram of stem	Kernel/(g•stem)	25.00
Thermal time at floral initiation stage	°Cd	500.00
Maximum grain size	g	0.04
Thermal time from the start grain filling stage to maturity	°Cd	400.00
Photoperiod sensitivity	-	2.50
Vernalization sensitivity	-	2.00

Note: APSIM, Agricultural Production Systems sIMulator. -, dimensionless.

2.3 Projections of future climate change

In this study, we projected future climate change for the five representative locations based on the monthly outputs of 29 GCMs from the Coupled Model Intercomparison Project Phase 5 (CMIP5) under two emission scenarios (RCP4.5 and RCP8.5) for three future time periods (2030s, 2050s and 2080s).

The Agricultural Model Intercomparison and Improvement Project (AgMIP) methodology (AgMIP, 2013) was used to downscale daily station-scale meteorological observations from the large-scale monthly outputs of GCMs. Using AgMIP downscaling approach, we projected daily future climate data based on the absolute change in minimum and maximum temperatures and relative change in rainfall in the climate model using the delta change method (Ruane et al., 2013; Kidanemariam et al., 2021). The detailed description on AgMIP methodology for downscaling and projecting was previously reported by AgMIP (2013). The projected climate conditions were put into the APSIM-wheat model to simulate wheat grain yield under future climate change scenarios. CO_2 concentrations under RCP4.5 and RCP8.5 scenarios in different future time periods can be found in Araya et al. (2015). Two future climate change scenarios were projected to justify the positive effect of CO_2 concentration on wheat grain yield. In one scenario, both CO_2 concentration and temperature were elevated, and in the other scenario, temperature was elevated with no elevation in CO_2 concentration.

2.4 Statistical analyses and uncertainty decomposition

Three sources of uncertainty were considered in projecting the impact of future climate change on wheat grain yield: climate models (29 GCMs), future climate change scenarios (RCPs_future time periods, including RCP4.5_2030s, RCP8.5_2030s, RCP4.5_2050s, RCP8.5_2050s, RCP4.5_2080s and RCP8.5_2080s), and five representative locations (Shiraz, Hamedan, Sanandaj, Kermanshah and Khorramabad). Variations that arose from the three sources of uncertainty were assessed using analysis of variance (ANOVA), which has been widely proposed in previous studies (Tao et al., 2018; Wang et al., 2018; Zhang et al., 2019). In the current study, three-way ANOVA (three factors as the sources of uncertainty) was used to estimate the main effects:

$$SST = SS_L + SS_G + SS_S + SS_L \times SS_G + SS_L \times SS_S + SS_G \times SS_S + SS_L \times SS_G \times SS_S + E, \quad (3)$$

where SST is the total sum of squares; SS_L is the sum of squares due to location; SS_G is the sum of squares due to GCM; SS_S is the sum of squares due to scenario; and E is the interaction effect among the factors.

All data analyses were performed using R statistical software, version 3.4.1 (R Core Team, 2017). The package "agricolae" was applied for data pre-processing and three-way ANOVA analysis.

3 Results

3.1 Projected future climate change

There was a great deal of variability in the baseline period (1980–2009) of seasonal mean temperature (October to June of the next year) and seasonal cumulative rainfall (October to June of the next year) among different climate types (Table 2). In the arid cold climate region, wheat crops experienced the highest seasonal mean temperature (15.11°C), while in the semi-arid cold regions, wheat crops completed growth with cooler weather (8.92°C). The five representative locations received 397.84 mm of seasonal cumulative rainfall on average during 1980–2009, ranging from 319.40 mm in the arid cold regions to 488.05 mm in the semi-arid cool regions.

At the five representative locations, compared to the baseline period, the seasonal mean temperature of multi-GCM ensembles was projected to increase by 0.50°C under RCP4.5 and 0.60°C under RCP8.5 in the near future (2030s) (Fig. 1a1–a5). In the middle future (2050s), the projected increase of seasonal mean temperature was 0.90°C under RCP4.5 and 1.30°C under RCP8.5. In the far future (2080s), the likely increase of seasonal mean temperature would be

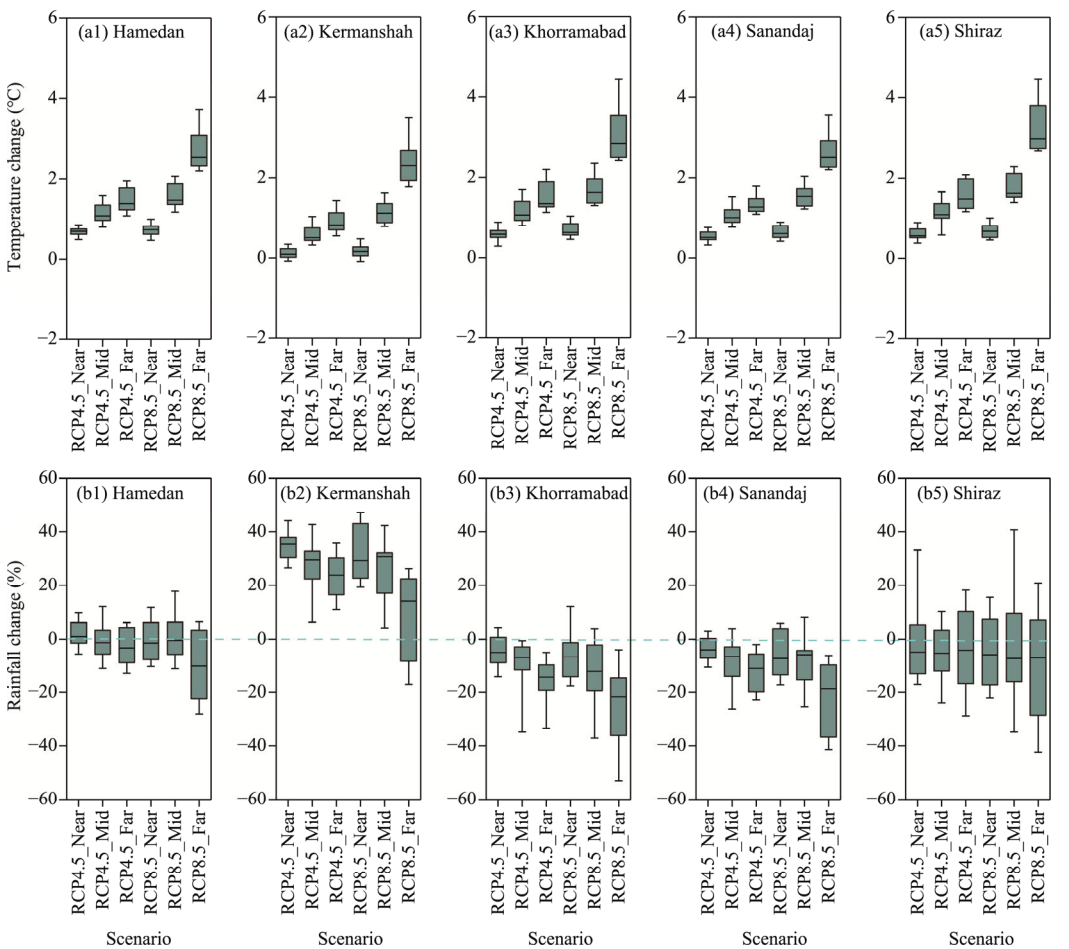

Fig. 1 Projected changes in future seasonal mean temperature (a) and seasonal cumulative rainfall (b) from 29 CMIP5 GCMs under RCP4.5 and RCP8.5 in the near future (2030s; RCP4.5_Near and RCP8.5_Near), middle future (2050s; RCP4.5_Mid and RCP8.5_Mid) and far future (2080s; RCP4.5_Far and RCP8.5_Far) compared to the baseline period (1980–2009) at the five representative locations. CMIP5, Coupled Model Intercomparison Project Phase 5; GCMs, General Circulation Models; RCP, Representative Concentration Pathway. Box boundaries indicate the 25th and 75th percentiles across GCMs, and whiskers below and above the box indicate the 10th and 90th percentiles, respectively. The black horizontal line within each box indicates the median of multi-GCM ensembles.

1.50°C under RCP4.5 and 2.60°C under RCP8.5, compared to the baseline period. Raising greenhouse gas emissions and lengthening the time periods (from the 2030s to the 2080s) enlarged the magnitude of rainfall change in the future compared to the baseline period. The change was defined from quantile 10 (Q10) to quantile 90 (Q90). When averaged across all the five representative locations, Q10–Q90 of multi-GCM ensembles for seasonal cumulative rainfall varied considerably under RCP4.5 (Fig. 1b1–b5). It hovered from –12.00% to 36.00% in the 2030s, from –17.00% to 29.00% in the 2050s, and from –22.00% to 25.00% in the 2080s. Under RCP8.5, the corresponding values ranged from –17.00% to 32.00% in the 2030s, from –24.00% to 31.00% in the 2050s, and from –41.00% to 19.00% in the 2080s. When averaged across all GCMs, RCPs and future time periods, the maximum and minimum increases in future seasonal mean temperature were respectively recorded in Shiraz (1.26°C) and Kermanshah (0.71°C) (Fig. 1a1–a5), where the climate is characterized by arid cold and semi-arid cool, respectively. The maximum change in seasonal cumulative rainfall was projected in Shiraz (–28.60% to 18.40%; arid cold climate), and the minimal change was projected in Hamedan (–13.90% to 10.20%; semi-arid cold climate) (Fig. 1b1–b5).

3.2 Projected future wheat grain yield

In the baseline period (1980–2009), the averaged wheat grain yield across all representative locations was 3.00 t/hm^2, with the maximum yield in Khorramabad (3.94 t/hm^2; semi-arid cool climate) and the minimum yield in Shiraz (2.60 t/hm^2; arid cold climate).

In future projections, the change trends of wheat grain yield for the different sets of GCMs, RCPs and future time periods were positive in all representative locations. When taken as a multi-GCM ensemble, the median of projected future wheat grain yield increased by 15.70% on average across all representative locations, RCPs and future time periods (Fig. 2a–e). Nevertheless, the magnitude of the increase was still dependent on locations, RCPs and future time periods. For example, across the five representative locations, 29 GCMs and two RCPs, projected future wheat grain yield was expected to increase by 12.30%, 17.10% and 17.70% in

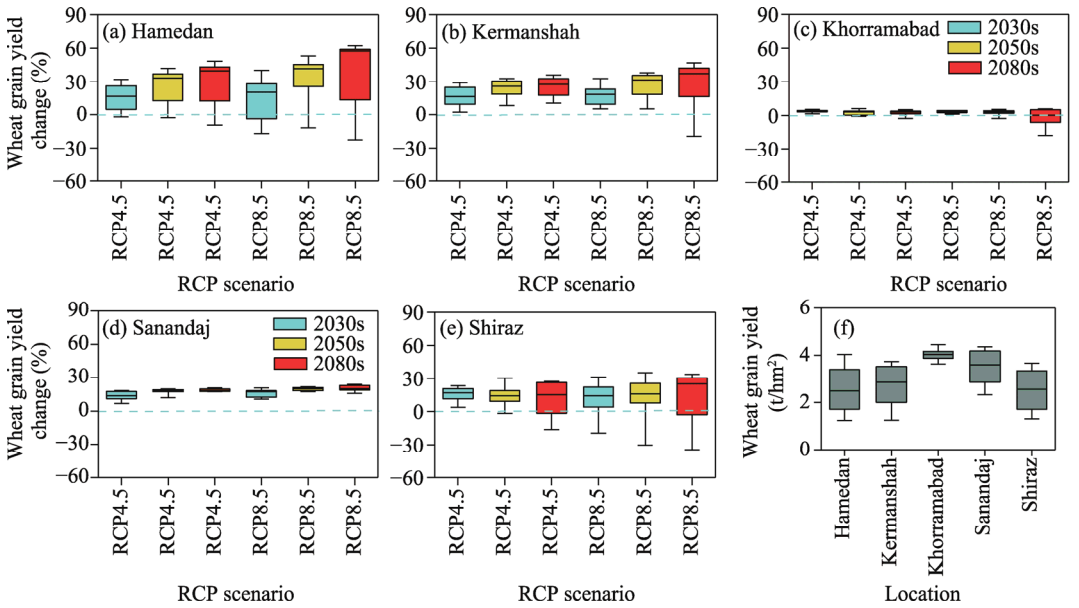

Fig. 2 Changes of projected future wheat grain yield from 29 CMIP5 GCMs under RCP4.5 and RCP8.5 in Hamedan (a), Kermanshah (b), Khorramabad (c), Sanandaj (d) and Shiraz (e) in the near future (2030s), middle future (2050s) and far future (2080s) compared to the baseline period (1980–2009), and the averaged wheat grain yields of the five representative locations in the baseline period (f). Box boundaries indicate the 25th and 75th percentiles across GCMs, and whiskers below and above the box indicate the 10th and 90th percentiles, respectively. The black horizontal line within each box indicates the median of multi-GCM ensembles.

the near future (2030s), middle future (2050s) and far future (2080s), respectively. Also, across the five representative locations, the median of projected future wheat grain yield of multi-GCM ensembles under RCP4.5 and RCP8.5 respectively increased by 17.80% and 20.20% in the 2080s, 17.70% and 20.00% in the 2040s, and 11.70% and 12.70% in the 2030s (Fig. 2a–e). As shown in Figures 2a–e and 3, the projected future wheat grain yield varied significantly at different locations. When averaged across all GCMs, RCPs and future time periods, the changes of projected future wheat grain yield ranged from –14.20% to 53.62% in Hamedan (semi-arid cold climate), and from –2.50% to 5.50% in Khorramabad (semi-arid cool climate) (Fig. 2a–e).

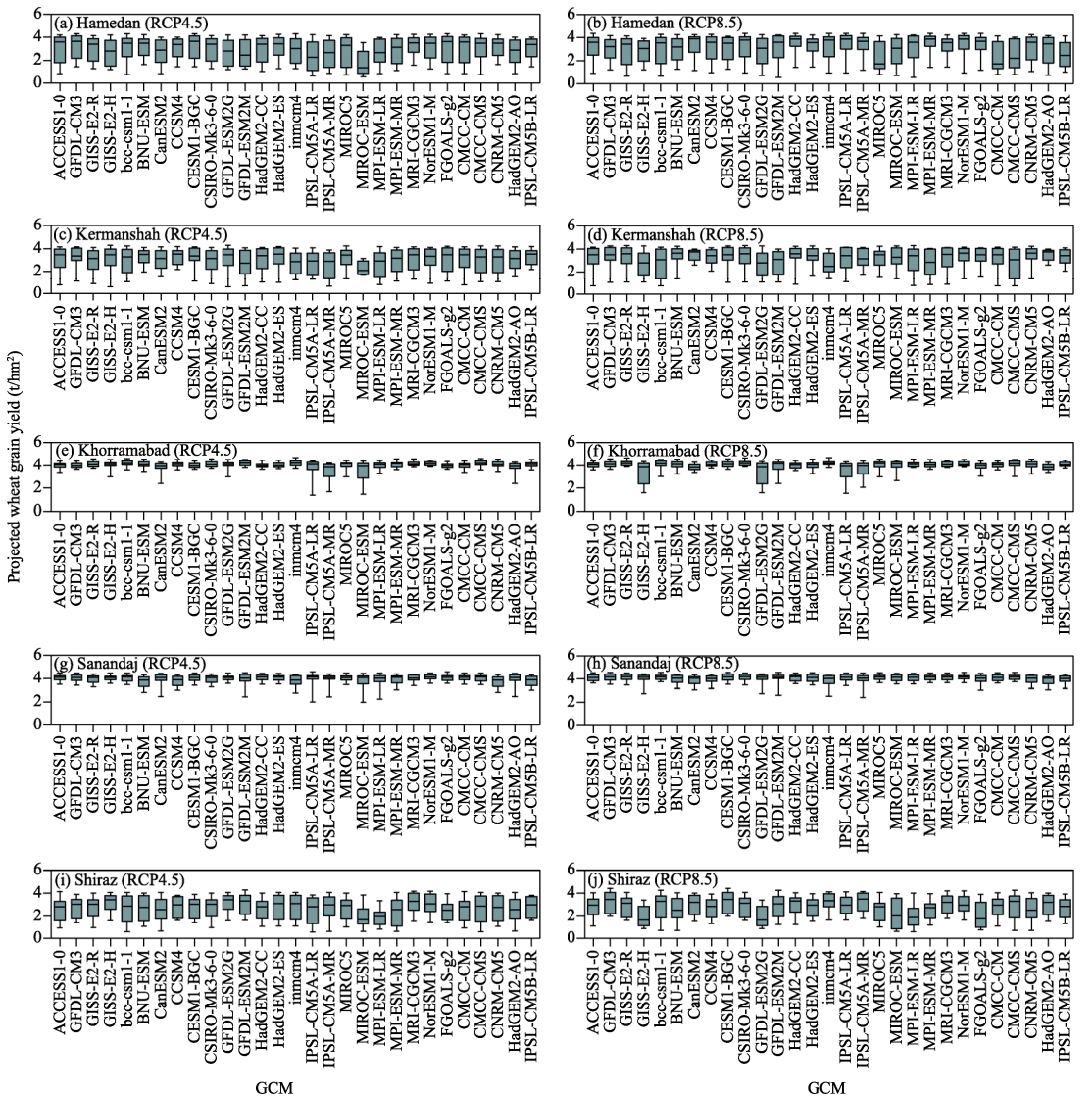

Fig. 3 Projected future wheat grain yield from 29 CMIP5 GCMs under RCP4.5 and RCP8.5 in Hamedan (a and b), Kermanshah (c and d), Khorramabad (e and f), Sanandaj (g and h) and Shiraz (i and j) in the middle future (2050s). Length of boxplot indicates the variability across years. Box boundaries indicate the 25th and 75th percentiles across years, and whiskers below and above the box indicate the 10th and 90th percentiles, respectively. The black horizontal line within each box indicates the median of multi-GCM ensembles.

The variability in projected future wheat grain yield was also affected by GCMs (length of boxplots in Fig. 2a–e). The greatest change in projected future wheat grain yield due to GCMs was observed under RCP8.5 in the 2080s in Hamedan, Kermanshah and Shiraz, while the minimal change was found under RCP4.5 in Khorramabad and Sanandaj (Fig. 2a–e). Figure 3

shows the projected future wheat grain yield using 29 GCMs under two RCPs for all representative locations in the middle future. It should be noted that only the 2050s timeline was included for simplicity. According to the results from 29 GCMs under two RCPs at all representative locations (Fig. 3), compared to the baseline period, the maximum change in future wheat grain yield was projected by the IPSL-CM5A-LR GCM (from –56.40% to 45.70%), whereas the minimum change was projected by the IPSL-CM5B-LR GCM (from –33.00% to 43.10%).

3.3 Relative contribution of the major sources of uncertainty in projected future wheat grain yield

Figure 4 indicates the total variance of the major sources of uncertainty in projected future wheat grain yield, which was partitioned into three major sources of uncertainty (locations, GCMs and scenarios (i.e., RCPs_future time periods)) and their interactions. As more than 97.22% of the variance was captured by locations, the share of each source of uncertainty associated with GCMs, scenarios and scenario×GCM was presented for each location separately (Fig. 4). As indicated in Figure 4, a large share of the variance (77.25%) was explained by scenarios at the semi-arid locations (e.g., 82.34% in Sanandaj, 78.61% in Hamedan, 75.51% in Kermanshah and 69.97% in Khorramabad). In contrast, at the arid location (Shiraz), the overall uncertainty from GCMs was great, such that 53.60% of the variance was explained by GCMs, followed by scenarios and scenario×GCM, explaining 32.39% and 14.01% of the variance, respectively. Interaction between scenarios and GCMs was the least important source of uncertainty at all locations. The uncertainty related to GCM×scenario was just 4.03% in Khorramabad, followed by 4.94% in Sanandaj, 5.49% in Hamedan, 6.47% in Kermanshah and 14.01% in Shiraz.

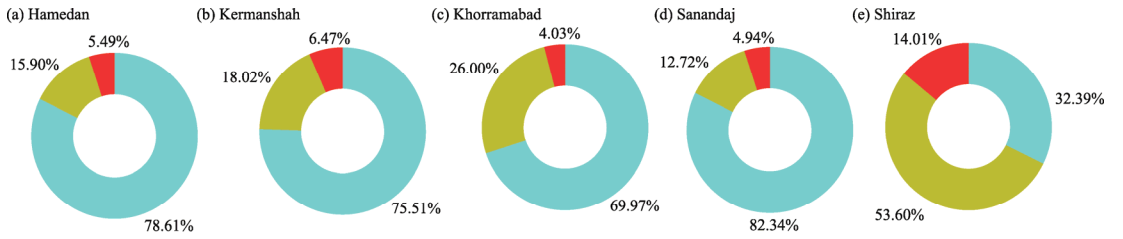

S.O.V.	*df*	MS	Variance fraction (%)
Locations	4	1.39E+09***	97.22
Scenarios	5	1.36E+07***	0.95
GCMs	28	8.77E+06***	0.61
Location×scenario	20	1.11E+07***	0.78
Location×GCM	112	2.57E+06***	0.18
Scenario×GCM	140	2.05E+06***	0.14
Location×scenario×GCM	560	7.72E+05***	0.05
Error	20, 872	8.75E+05***	0.06

Fig. 4 Analysis of variance (ANOVA) for projected future wheat grain yield as affected by locations, scenarios (RCPs_future time periods) and GCMs, as well as their interactions. The share of the uncertainty related to scenarios, GCMs and their interactions (scenario×GCM) for the projected future wheat grain yield are presented in donut charts. (a), Hamedan; (b), Kermanshah; (c), Khorramabad; (d), Sanandaj; (e), Shiraz. S.O.V., sources of variation; *df*, degrees of freedom; MS, mean of squares; ***, significant at the 0.001 probability level.

4 Discussion

4.1 Changes in projected future wheat grain yield and its associated uncertainty

In the baseline period (1980–2009), the maximum and minimum wheat grain yields were recorded in Khorramabad (3.94 t/hm^2) with a semi-arid cool climate and Shiraz (2.60 t/hm^2) with an arid cold climate, respectively (Fig. 2f). This can be related to cumulative rainfall during the

wheat growing season, i.e., wheat crops received more seasonal rainfall in Khorramabad (409.60 mm) than in Shiraz (319.40 mm) (Table 2). Figure 2a–e indicated that projected future wheat grain yield increased under different RCPs and future time periods at all representative locations. This increase was largely associated with the rise in CO_2 concentrations projected in the future (Fig. 5a1–a5). In fact, as previously discussed in similar areas (e.g., Lv et al., 2013; Amiri et al., 2021), the positive effect of CO_2 fertilization can offset the negative impact of rising temperature on wheat grain yield increase. The positive effect of CO_2 fertilization varied considerably across the five representative locations. For example, wheat grain yield received the least positive effect from CO_2 emission in Khorramabad in the future period (Figs. 2c and 5a3). The length of the wheat growth period decreased more in Khorramabad (decreased by 9.38%) than at the other four representative locations (decreased by 0.97% to 8.64%) under rising temperature conditions (Fig. 5b1–b5), since rising temperature can reduce the length of the wheat growing season. Many scientific reports worldwide have also indicated the negative effect of rising temperature on the length of the crop growing season, and consequently crop grain yield (Asseng et al., 2014;

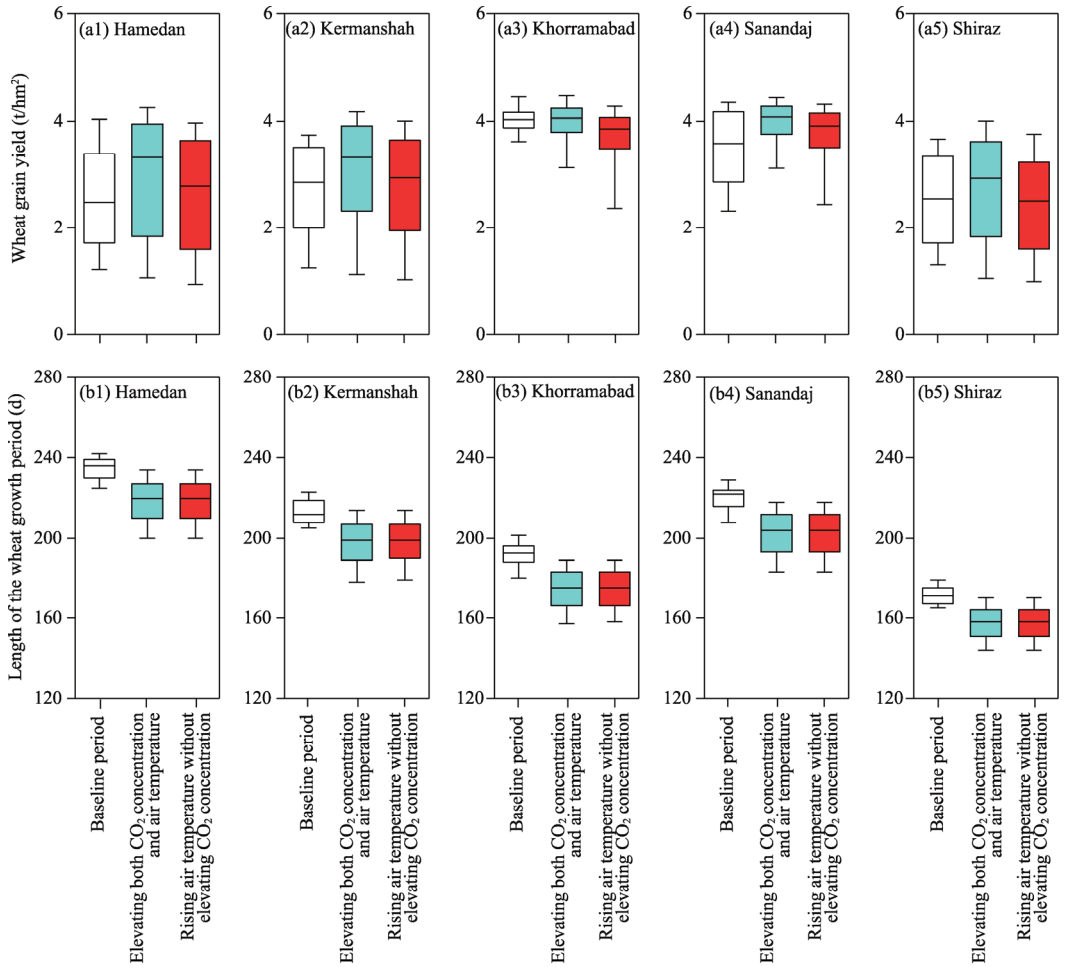

Fig. 5 Projected wheat grain yield (a1–a5) and the length of the wheat growth period (b1–b5) at the five representation locations in the baseline period and in the future under two climate change scenarios: elevating both CO_2 concentration and temperature (blue boxes); and only rising temperature without elevating CO_2 concentration (red boxes). (a1 and b1), Hamedan; (a2 and b2), Kermanshah; (a3 and b3), Khorramabad; (a4 and b4), Sanandaj; (a5 and b5), Shiraz. The length of boxplots indicates the variability among the 29 CMIP5 GCMs. Box boundaries indicate the 25th and 75th percentiles across GCMs, and whiskers below and above the box indicate the 10th and 90th percentiles, respectively. The black horizontal line within each box indicates the median of multi-GCM ensembles.

Rahimi-Moghaddam et al., 2019; Ding et al., 2021).

Specifically, the projection results in the current study indicated that great variation in wheat grain yield would occur in the future according to locations, RCPs, future time periods and GCMs (Figs. 2 and 3). As shown in Figure 4, a much higher variance was explained by locations, compared to scenarios and GCMs, which may be due to the large differences in annual cumulative rainfall (from 265.00 mm in Hamedan to 569.10 mm in Kermanshah) and annual mean temperature (ranging from 11.46°C in Hamedan to 18.32°C in Shiraz) of the five representative locations (Table 2). In addition, the variation in future wheat grain yield was higher at locations with less rainfall (Fig. 2). The highest variation was recorded in Hamedan (Fig. 2), which typically receives less rainfall (265.00 mm) than the other locations (320.90–569.10 mm) (Table 2). Indeed, rainfall plays a much greater role in grain yield change than temperature in dryland environments. In the future, for a specific area with low rainfall, even a tiny variation in rainfall could cause much larger changes in wheat grain yield (Schierhorn et al., 2020). For instance, Hamedan with a semi-arid cold climate had a much lower annual mean temperature (11.46°C) than Shiraz with an arid cold climate (18.32°C) (Table 2), while the change of future wheat grain yield was much larger in Hamedan than in Shiraz (Fig. 2), mainly because of less rainfall in Hamedan (265.00 mm) than in Shiraz 320.90 mm (Table 2). In a study assessing the impact of climate variability on crop yield and irrigated water demand in South Asia (Ahmad et al., 2020), it was reported that in the absence of irrigation, up to 39.00% of the variation in wheat grain yield and 75.00% of the variation in rice yield were associated with rainfall changes at all study locations. Another research (Gupta and Mishra, 2019) investigated the uncertainty of rice yield in agro-ecological zones of India and highlighted that high temperature and low rainfall may be the reason for the great variation in yield in some agro-ecological zones in West India.

In this study, projected seasonal mean temperature and seasonal cumulative rainfall varied substantially with the GCMs and scenarios used, indicating strong uncertainty for future climate conditions in the study area. The proportion of uncertainty, however, differed among scenarios, GCMs and locations. The highest proportion in all cases was associated with the 29 GCMs and the five representative locations (length of boxplots in Figs. 2a–e and 3). In the arid climate zone (i.e., Shiraz), GCMs showed the largest contribution to the uncertainty in projecting future wheat grain yield, followed by scenarios (Fig. 4). This is likely due to the high variations in projected seasonal cumulative rainfall among GCMs (Fig. 1b1–b5) in combination with a higher increase in future temperature compared to other locations. It is also interesting to note that the uncertainty resulting from GCMs at different representative locations was magnified with increasing emission scenarios (from RCP4.5 to RCP8.5) and farther time periods (from 2030s to 2080s), particularly for rainfall projections. In agreement with these findings, Wang et al. (2018) reported that climate projections from GCMs contributed to a large difference in wheat yield, especially in dryland regions of eastern Australia. In their study, GCMs were the largest source of uncertainty in projecting the change of wheat grain yield. Another study has also indicated that a large variation in temperature projection due to GCMs and scenarios would be of importance in affecting crop yield variability in the future (Asseng et al., 2011). Specifically, Asseng et al. (2011) reported that observed variations in the average growing season temperature of ±2.00°C from 1996 to 2007 in the main wheat growing regions of Australia have caused a reduction in grain production of up to 50.00%. Previous studies have also showed that GCMs and scenarios are the major sources of uncertainty in quantifying the impact of climate change, as GCMs have limited capacity for predicting climate extremes and inter-annual climate variations, which would ultimately lead to false representation of the impact of climate change on crop yield (Osborne et al., 2013; Asseng et al., 2014; Araya et al., 2015; Kassie et al., 2015). This is related to the structure of GCMs, particularly when GCMs are applied to project the future conditions of various regions with contrasting climate types (warm-dry, cool-dry, warm-wet, cool-wet and temperate) located at different altitudes (Ruane and McDermid, 2017; Ahmad et al., 2020). Therefore, the ensemble use of a wide range of GCMs should be prioritized to narrow the uncertainty when assessing wheat grain yield under future climate change, particularly in dryland environments characterized by

large fluctuations in rainfall and temperature.

Moreover, scenarios (RCP×future time period) made an important contribution to the uncertainty in projecting future wheat grain yield changes at all semi-arid climate locations (i.e., Hamedan, Sanandaj, Kermanshah and Khorramabad), and higher rainfall along with elevated CO_2 concentration has resulted in a considerable increase in wheat grain yield compared to arid climate location (Fig. 2). These findings are in accordance with those of Masutomi et al. (2009), who pointed out that a higher CO_2 concentration may bring higher uncertainty in projecting the effect of climate change on rice yield in the 2080s in Southeast Asia, and the average change of rice production varied with and without CO_2 fertilization, across all scenarios and GCMs.

The current findings further revealed that the GCMs of the IPSL-CM5A-LR, IPSL-CM5A-MR, MIROC-ESM, CanESM2 and HadGEM2-AO contributed substantially to the total uncertainty in projecting the impact of climate change on wheat grain yield, while the IPSL-CM5B-LR, CCSM4 and BNU-ESM made moderate effects and can be used to project the future climate conditions of similar environments worldwide, especially in the absence of computational facility capable of processing large amounts of data obtained from simulation experiments (GCM×RCP×future time period×location) (Fig. 3). Overall, GCMs and scenarios have been determined to be the major sources of uncertainty in projecting the impact of climate change on wheat growth and grain yield. The magnitude of the uncertainty, however, is highly dependent upon climate.

4.2 Limitations

The current study aimed to assess the major sources of uncertainty (GCMs, locations and scenarios) in projecting the impact of climate change on wheat grain yield. However, there are many other sources of uncertainty when investigating the impact of climate change on crop production, including crop models (e.g., model inputs, model parameters and model structure) (Asseng et al., 2013), downscaling approaches (Khan et al., 2006), genotypes and management options (e.g., irrigation regime, nitrogen application and sowing date) (Ojeda et al., 2021), and soil types (e.g., plant available water capacity) (Wang et al., 2018). For example, a review study of 277 articles from 1991 to 2019 in 82 countries (460 locations) across all continents reported that articles with the uncertainty in projecting the impact of climate change on crop yield related to model parameters and model structure comprised 28.00% and 20.00% of the studies, respectively (Chapagain et al., 2022). In another study, using the APSIM, MONICA (Model for Nitrogen and Carbon in Agro-ecosystems) and SIMPLACE (Scientific Impact Assessment and Modelling Platform for Advanced Crop and Ecosystem Management) crop models, Kamali et al. (2022) investigated the main drivers of uncertainty regarding management practices (water allocation strategies, three sowing dates and three maize cultivars) in projecting irrigated maize yield under historical conditions as well as under the scenarios of rising temperature and altered irrigation water availability in southern Spain. They concluded that irrigation strategy was the main driver of uncertainty in projecting crop yield (accounting for 66.00% of the variance). They also reported that under rising temperature, both crop model and cultivar choice contributed to the uncertainty in projecting crop yield as important as irrigation strategy. Generally, studies that focused on uncertainty in all parameters and inputs simultaneously are still lacking (Chapagain et al., 2022). It should also be mentioned that the current research was conducted only under water-limited conditions. Other factors such as nitrogen (Wang et al., 2018) and phosphorus (Engebretsen et al., 2019) can also affect the uncertainty of projected wheat grain yield in the future. Accordingly, it is suggested that the simultaneous effects of all environmental (i.e., soil and climate), genetic and management (e.g., sowing date, plant density, irrigation and nitrogen fertilizer) factors should be considered when analyzing the sources of uncertainty in projecting future wheat grain yield.

5 Conclusions

In this study, we quantified three sources of uncertainty in projecting future wheat grain yield under climate change based on 29 GCMs, six scenarios (RCP4.5_2030s, RCP8.5_2030s,

RCP4.5_2050s, RCP8.5_2050s, RCP4.5_2080s and RCP8.5_2080s) and five representative locations with different climate types (Shiraz, Hamedan, Sanandaj, Kermanshah and Khorramabad). Our results indicated that the increase in projected future wheat grain yield under different RCPs in different future time periods at all representative locations was largely associated with the rise in CO_2 concentration in the upcoming periods.

Most of the variations in projected future wheat grain yield can be explained by locations, followed by scenarios and GCMs, depending on the climate of each location. At the arid climate location (Shiraz), the biggest source of uncertainty in predicting future wheat grain yield was associated with GCMs, mainly due to high variations in projected seasonal cumulative rainfall among GCMs. Accordingly, it seems that multi-GCM ensembles should be given priority to adequately address and reduce the uncertainty when projecting wheat grain yield under climate change conditions, particularly in arid climate regions. At all semi-arid climate locations (Hamedan, Sanandaj, Kermanshah and Khorramabad), scenarios were the biggest source of uncertainty in projecting future wheat grain yield changes. Our findings also revealed that the IPSL-CM5B-LR, CCSM4 and BNU-ESM made moderate effects in projecting the impact of climate change on wheat grain yield and can be used to project future climate conditions of similar environments worldwide, especially in the absence of computational facility capable of processing large amounts of data obtained from simulation experiments (GCM×RCP×future time period×location). Furthermore, only one crop model (APSIM-wheat model) was used in the current study to simulate the impact of climate change on wheat grain yield. Accordingly, some potential sources of uncertainty resulting from crop models (such as model structure and model parameters), downscaling approaches, adaptation options (irrigation regime, nitrogen application, sowing date and cultivar) and soils should be taken into account in future studies. It is worth noting that calibrating the crop models for the effects of CO_2 on photosynthesis and transpiration of the local cultivar is of importance, as there is evidence of widespread genotypic variability in the response of those processes to CO_2.

Acknowledgements

The project was funded by the Deputy of Research Affairs, Lorestan University, Iran (Contract No. 1400-6-02-5-18-1402).

References

AgMIP. 2013. Guide for running AgMIP climate scenario generation tools with R in Windows Version 2.3. [2022-04-18]. https://raw.githubusercontent.com/agmip/Climate-Scenarios-Generator/master/Guide-for-Running-AgMIP-Climate-Scenario-Generation-with-R-v2.0.pdf

Ahmad I, Ahmad B, Boote K, et al. 2020. Adaptation strategies for maize production under climate change for semi-arid environments. European Journal of Agronomy, 115: 126040, doi: 10.1016/j.eja.2020.126040.

Ahmad Q U A, Biemans H, Moors E, et al. 2020. The impacts of climate variability on crop yields and irrigation water demand in South Asia. Water, 13(1): 50, doi: 10.3390/w13010050.

Amiri S, Eyni-Nargeseh H, Rahimi-Moghaddam S, et al. 2021. Water use efficiency of chickpea agro-ecosystems will be boosted by positive effects of CO_2 and using suitable genotype×environment×management under climate change conditions. Agricultural Water Management, 252: 106928, doi: 10.1016/j.agwat.2021.106928.

Amiri S R, Deihimfard R, Soltani A. 2016. A single supplementary irrigation can boost chickpea grain yield and water use efficiency in arid and semiarid conditions: a modeling study. Agronomy Journal, 108(6): 2406–2416.

Araya A, Hoogenboom G, Luedeling E, et al. 2015. Assessment of maize growth and yield using crop models under present and future climate in southwestern Ethiopia. Agricultural and Forest Meteorology, 214: 252–265.

Asseng S, Foster I, Turner N C. 2011. The impact of temperature variability on wheat yields. Global Change Biology, 17(2): 997–1012.

Asseng S, Ewert F, Rosenzweig C, et al. 2013. Uncertainty in simulating wheat yields under climate change. Nature Climate Change, 3(9): 827–832.

Asseng S, Ewert F, Martre P, et al. 2014. Rising temperatures reduce global wheat production. Nature Climate Change, 5:

143–147.

Boughton W C. 1989. A review of the USDA SCS curve number method. Soil Research, 27(3): 511–523.

Chapagain R, Remenyi T A, Harris R M, et al. 2022. Decomposing crop model uncertainty: A systematic review. Field Crops Research, 279: 108448, doi: 10.1016/j.fcr.2022.108448.

Cheng L, Phillips T J, AghaKouchak A. 2015. Non-stationary return levels of CMIP5 multi-model temperature extremes. Climate Dynamics, 44(11): 2947–2963.

Collins B, Najeeb U, Luo Q, et al. 2022. Contribution of climate models and APSIM phenological parameters to uncertainties in spring wheat simulations: Application of SUFI-2 algorithm in northeast Australia. Journal of Agronomy and Crop Science, 208(2): 225–242.

De Pauw E, Ghasemi Dehkordi V R, Ghaffari A. 2018. Agroecological zones. In: Roozitalab M, Siadat H, Farshad A. The Soils of Iran. Enschede: Springer, Cham, 163–173.

Ding Z L, Ali E F, Elmahdy A M, et al. 2021. Modeling the combined impacts of deficit irrigation, rising temperature and compost application on wheat yield and water productivity. Agricultural Water Management, 244: 106626, doi: 10.1016/j.agwat.2020.106626.

Edenhofer O. 2014. Climate Change 2014: Mitigation of Climate Change: Working Group III Contribution to the IPCC Fifth Assessment Report. New York: Cambridge University Press, 1–1435.

Eghdamirad S, Johnson F, Sharma A. 2017. Using second-order approximation to incorporate GCM uncertainty in climate change impact assessments. Climate Change, 142(1–2): 37–52.

Engebretsen A, Vogt R D, Bechmann M. 2019. SWAT model uncertainties and cumulative probability for decreased phosphorus loading by agricultural Best Management Practices. CATENA, 175: 154–166.

FAO (Food and Agriculture organization of the United Nations). 2020. FAOSTAT Data. [2022-04-18]. http://www.fao.org/faostat/en/#data/QC.

Freychet N, Hegerl G, Mitchell D, et al. 2021. Future changes in the frequency of temperature extremes may be underestimated in tropical and subtropical regions. Communications Earth & Environment, 2(1): 1–8.

Gupta R, Mishra A. 2019. Climate change induced impact and uncertainty of rice yield of agro-ecological zones of India. Agricultural Systems, 173: 1–11.

Hao S R, Ryu D, Western A, et al. 2021. Sensitivity analysis of APSIM wheat yield predictions. American Geophysical Union, New Orleans (USA). 2021-12-12–2021-12-17. New Orleans, USA.

Hawkins E, Smith R S, Gregory J M, et al. 2016. Irreducible uncertainty in near-term climate projections. Climate Dynamics, 46(11): 3807–3819.

Hawkins R H, Ward T J, Woodward D, et al. 2008. Curve Number Hydrology: State of Practice. Reston: American Society of Civil Engineers, 1–104.

Holzworth D P, Huth N I, deVoil P G, et al. 2014. APSIM-evolution towards a new generation of agricultural systems simulation. Environmental Modelling & Software, 62: 327–350.

Hosseinzadehtalaei P, Tabari H, Willems P. 2017. Uncertainty assessment for climate change impact on intense precipitation: how many model runs do we need? International Journal of Climatology, 37(S1): 1105–1117.

Kamali B, Lorite I J, Webber H A, et al. 2022. Uncertainty in climate change impact studies for irrigated maize cropping systems in southern Spain. Scientific Reports, 12: 4049, doi: 10.1038/s41598-022-08056-9.

Kassie B T, Asseng S, Rotter R P, et al. 2015. Exploring climate change impacts and adaptation options for maize production in the Central Rift Valley of Ethiopia using different climate change scenarios and crop models. Climatic Change, 129(1): 145–158.

Khan M S, Coulibaly P, Dibike Y. 2006. Uncertainty analysis of statistical downscaling methods. Journal of Hydrology, 319(1–4): 357–382.

Kidanemariam S, Goitom H, Desta Y. 2021. Coupled application of R and WetSpa models for assessment of climate change impact on streamflow of Werie Catchment, Tigray, Ethiopia. Journal of Water and Climate Change, 12(3): 916–936.

Liu W H, Ye T, Jägermeyr J, et al. 2021. Future climate change significantly alters interannual wheat yield variability over half of harvested areas. Environmental Research Letters, 16(9): 094045, doi: 10.1088/1748-9326/ac1fbb.

Lobell D B, Hammer G L, Chenu K, et al. 2015. The shifting influence of drought and heat stress for crops in northeast Australia. Global Change Biology, 21(11): 4115–4127.

Lv Z F, Liu X J, Cao W X, et al. 2013. Climate change impacts on regional winter wheat production in main wheat production regions of China. Agricultural and Forest Meteorology, 171–172: 234–248.

Masutomi Y, Takahashi K, Harasawa H, et al. 2009. Impact assessment of climate change on rice production in Asia in comprehensive consideration of process/parameter uncertainty in general circulation models. Agriculture, Ecosystems & Environment, 131(3–4): 281–291.

Obembe O S, Hendricks N P, Tack J. 2021. Decreased wheat production in the USA from climate change driven by yield losses rather than crop abandonment. PLOS ONE, 16(6): e0252067, doi: 10.1371/journal.pone.0252067.

Ojeda J J, Rezaei E E, Kamali B, et al. 2021. Impact of crop management and environment on the spatio-temporal variance of potato yield at regional scale. Field Crops Research, 270: 108213, doi: 10.1016/j.fcr.2021.108213.

Olesen J E, Carter T R, Diaz-Ambrona C H, et al. 2007. Uncertainties in projected impacts of climate change on European agriculture and terrestrial ecosystems based on scenarios from regional climate models. Climatic Change, 81(1): 123–143.

Osborne T, Rose G, Wheeler T. 2013. Variation in the global-scale impacts of climate change on crop productivity due to climate model uncertainty and adaptation. Agricultural and Forest Meteorology, 170: 183–194.

Ponce V M, Hawkins R H. 1996. Runoff curve number: Has it reached maturity? Journal of Hydrologic Engineering, 1(1): 11–19.

R Core Team. 2017. R: A Language and Environment for Statistical Computing. Online: R Foundation for Statistical Computing, Vienna, Austria. [2022-04-18]. http://www.R-project.orgs.

Rahimi-Moghaddam S, Kambouzia J, Deihimfard R. 2019. Optimal genotype×environment×management as a strategy to increase grain maize productivity and water use efficiency in water-limited environments and rising temperature. Ecological Indicators, 107: 105570, doi: 10.1016/j.ecolind.2019.105570.

Rahimi-Moghaddam S, Deihimfard R, Azizi K, et al. 2021. Characterizing spatial and temporal trends in drought patterns of rainfed wheat (*Triticum aestivum* L.) across various climatic conditions: A modelling approach. European Journal of Agronomy, 129: 126333, doi: 10.1016/j.eja.2021.126333.

Rahman M H, Ahmad A, Wang X C, et al. 2018. Multi-model projections of future climate and climate change impacts uncertainty assessment for cotton production in Pakistan. Agricultural and Forest Meteorology, 253–254: 94–113.

Rettie F M, Gayler S, Weber T K D, et al. 2022. Climate change impact on wheat and maize growth in Ethiopia: A multi-model uncertainty analysis. PLOS ONE, 17(1): e0262951, doi: 10.1371/journal.pone.0262951.

Reyenga P J, Howden S M, Meinke H, et al. 1999. Modelling global change impacts on wheat cropping in south-east Queensland, Australia. Environmental Modelling & Software, 14(4): 297–306.

Ruane A C, Cecil L D, Horton R M, et al. 2013. Climate change impact uncertainties for maize in Panama: Farm information, climate projections, and yield sensitivities. Agricultural and Forest Meteorology, 170: 132–145.

Ruane A C, McDermid S P. 2017. Selection of a representative subset of global climate models that captures the profile of regional changes for integrated climate impacts assessment. Earth Perspectives, 4(1): 1–20.

Ruiz-Ramos M, Rodríguez A, Dosio A, et al. 2016. Comparing correction methods of RCM outputs for improving crop impact projections in the Iberian Peninsula for 21st century. Climatic Change, 134(1–2): 283–297.

Saddique Q, Liu D L, Wang B, et al. 2020. Modelling future climate change impacts on winter wheat yield and water use: A case study in Guanzhong Plain, northwestern China. European Journal of Agronomy, 119: 126113, doi: 10.1016/j.eja.2020.126113.

Saxton K E, Willey P H. 2005. The SPAW model for agricultural field and pond hydrologic simulation. In: Singh V P, Frevert D K. Watershed Models. Boca Raton: CRC Press, 400–435.

Schierhorn F, Hofmann M, Adrian I, et al. 2020. Spatially varying impacts of climate change on wheat and barley yields in Kazakhstan. Journal of Arid Environments, 178: 104164, doi: 10.1016/j.jaridenv.2020.104164.

Shi L J, Feng P Y, Wang B, et al. 2020. Quantifying future drought change and associated uncertainty in southeastern Australia with multiple potential evapotranspiration models. Journal of Hydrology, 590: 125394, doi: 10.1016/j.jhydrol.2020.125394.

Tao F L, Rötter R P, Palosuo T, et al. 2018. Contribution of crop model structure, parameters and climate projections to uncertainty in climate change impact assessments. Global Change Biology, 24(3): 1291–1307.

UNEP (United Nations Environment Programme). 1992. World Atlas of Desertification. [2022-04-18]. https://wedocs.unep.org/20.500.11822/42137.

UNESCO (United Nations Educational, Scientific and Cultural Organization). 1979. Map of the World Distribution of Arid Regions: Explanatory Note. Paris: UNESCO, 1–54.

Vogeler I, Sharp J, Cichota R, et al. 2022. Sensitivity analysis of soil parameters in the Agricultural Production Systems sIMulator (APSIM). Soil Research, 61(2): 176–186.

Wang B, Liu D L, Waters C, et al. 2018. Quantifying sources of uncertainty in projected wheat yield changes under climate change in eastern Australia. Climatic Change, 151(2): 259–273.

Zhang Y, Zhao Y X, Feng L P. 2019. Higher contributions of uncertainty from global climate models than crop models in maize-yield simulations under climate change. Meteorological Applications, 26(1): 74–82.

Zhao G, Bryan B A, Song X D. 2014. Sensitivity and uncertainty analysis of the APSIM-wheat model: Interactions between cultivar, environmental, and management parameters. Ecological Modelling, 279: 1–11.

Appendix

Table S1 Summarized results of APSIM model evaluation (adapted from Rahimi-Moghaddam et al., 2021)

Trait	R^2	*d*-index	nRMSE (%)	MBE	*N*
Days to flowering (d)	0.99	0.96	3.180	4.000	9
Days to maturity (d)	0.99	0.97	2.150	1.880	9
Grain yield (t/hm^2)	0.88	0.99	12.300	–0.105	55
Soil moisture (cm^3/cm^3)	0.99	0.93	8.700	0.002	56

Note: R^2, coefficient of determination; *d*-index, Wilmot's index of agreement; nRMSE, normalized root mean square error; MBE, mean bias error; N, number of observations.